

RESEARCH ARTICLE

Antioxidant Activities Exhibited by Benzofuran-1, 3-Thiazolidin-4- one Derivative: A Theoretical Study

Fella Ati^{1,4}, Soraya Abtouche¹, Ahmed Chergui², Hassan Y. Aboul-Enein³, Boubekeur Maouche¹ and Meziane Brahimi^{1,*}

¹Laboratory of Theoretical Physico Chemistry and Computational Chemistry, Faculty of Chemistry, USTHB, BP N° 32 El Alia, 16111, Algiers, Algeria.

²Faculty of Chemistry, USTHB, BP N° 32 El Alia 16111, Algiers, Algeria.

³Medicinal and Pharmaceutical Chemistry Department, Pharmaceutical and Drug Industries Research Division, National Research Centre, Cairo 12622, Egypt

⁴Department of Chemistry, Faculty of Sciences, University Saad Dahlab BLIDA 1, Algiers, Algeria

*Corresponding author: Meziane Brahimi Laboratory of Theoretical Physico Chemistry and Computational Chemistry, Faculty of Chemistry, USTHB, BP N° 32 El Alia, 16111, Algiers, Algeria. Email : mez_brahimi@yahoo.fr

Citation: Meziane Brahimi, Ati Fella, Abtouche Soraya, Chergui Ahmed, Aboul-Enein Hassan Y, Maouche Boubekeur (2023) Antioxidant Activities Exhibited by Benzofuran-1, 3-Thiazolidin-4- One Derivative : A Theoretical Study. J Med Chem Drug Design 1: 103

Abstract

The free radical scavenging activity of the benzofuran Schiff base and thiazolidinone derivatives were studied using the density functional theory (DFT) method. Three main reaction mechanisms were explored: hydrogen atom transfer (HAT), single-electron transfer followed by proton transfer (SET-PT), and sequential proton loss electron transfer (SPLET). The thermodynamic descriptors associated with these mechanisms were calculated in the gas phase and solvents. Our results indicate that compounds **3a**, **3c**, **3f**, **4d**, and **4e** have a potential for free radical scavenging via the three mechanisms. The results show that HAT is proposed as a thermodynamically preferred mechanism in the gas phase and non-polar solutions, while SPLET is preferred in polar environments.

Moreover, the electron-withdrawing groups (EWG) attached to π conjugated groups at the N position of the benzofuran derivatives decrease bond dissociation enthalpies (BDEs) and electron-donating groups (EDG) are helpful to decrease the ionization potential (IPs). Moreover, the MLR statistical analyses lead to a good correlation between the IC_{50} (μ M) and ionization potential (IP), proton dissociation enthalpy (PDE), proton affinity (PA), and the electron transfer enthalpy (ETE) descriptor. Calculation of the ADME properties shows that compounds 1a, 2a, 2b, 3a, and 4a possess the biocompatibility criteria.

Keywords: Benzofuran Thiazolidinone Derivatives; Antioxidant Activity; Benzofuran Derivatives; DFT, MLR Studies

Introduction

Reactive oxygen species (ROS) and reactive nitrogen species (RNS) are the by-products of the cellular redox process and are well documented to play a dual role as deleterious and beneficial species. The overproduction of these species leads to oxidative stress, which is a state in which the biological system is unable to ensure the oxidant-antioxidant equilibrium [1]. Oxidative stress causes irreversible damage to cells, lipids, membranes, proteins, and DNA. It is also involved in premature aging and major diseases, including cancer, Alzheimer's disease, autism, HIV infection, and cerebrovascular accidents [2, 3]. In a normal physiological environment, the generation of reactive species is closely regulated by different enzymatic and non enzymatic antioxidants. Antioxidants are substances that can scavenge free radicals by donating a hydrogen atom or an electron to chelate redox-active metals and inhibit lipoxygenases [4, 5]. To search for new antioxidants, Benzofuran is one of the most important heterocycles containing oxygen [6]. Many benzofuran derivatives, such as benzofuran 1, 3-thiazolidin-4-ones display potent biological and pharmacological activities, such as anti-Alzheimer's, anti-dermal, anti-hyperglycemic, anti-inflammatory, β -adrenoceptor antagonistic [7], anti-microbial, anti-pyretic, anti-tumor, immunosuppressive [8-11], and especially antiviral activities [12-13], anthelmintic, anti-histaminic, anti-hyperlipidemic, anti-bacterial, anti-convulsant, anti-proliferative, anti-tubercular, anti-diabetic, anti-fungal, cardiovascular, follicle-stimulating hormone receptor agonist, hypnotic as published in several research articles [14-16] and anti-viral activities as well [17-20].

The synthesis of new benzofuran (benzofuran-thiazole, benzofuran-azo, benzofuran-hydrazo, and benzofuran-piperazine hybrids) as antitumor agents [21] or bis(benzofuran-thiazolidinone)s and bis(benzofuran-thiazinanone)s as inhibiting agents for Chikungunya virus [22] continues to increase. Iminosubstituted (**3a-3f**) and 1, 3-thiazolidinone (**4a-4f**) substituted benzofuran derivatives (see Figure. 1) were recently screened for radical scavenging activity by Latif et al., 2013, through 2, 2-diphenyl-1-picrylhydrazyl (DPPH) assay [23]. Initial results indicate that the antioxidant response of the khellin (**1a**) and its hydrolyzed derivatives (**2a**, **2b**) is poor while the 1,3-benzofuran derivatives (**3c**, **3d**, **3f**) and (**4d**) proved to have almost similar antioxidant activity with EC_{50} values 10.59, 9.72, 8.57 and 8.27 μ M respectively, and is comparable to that of standard drug Trolox (5.42 μ M) [24].

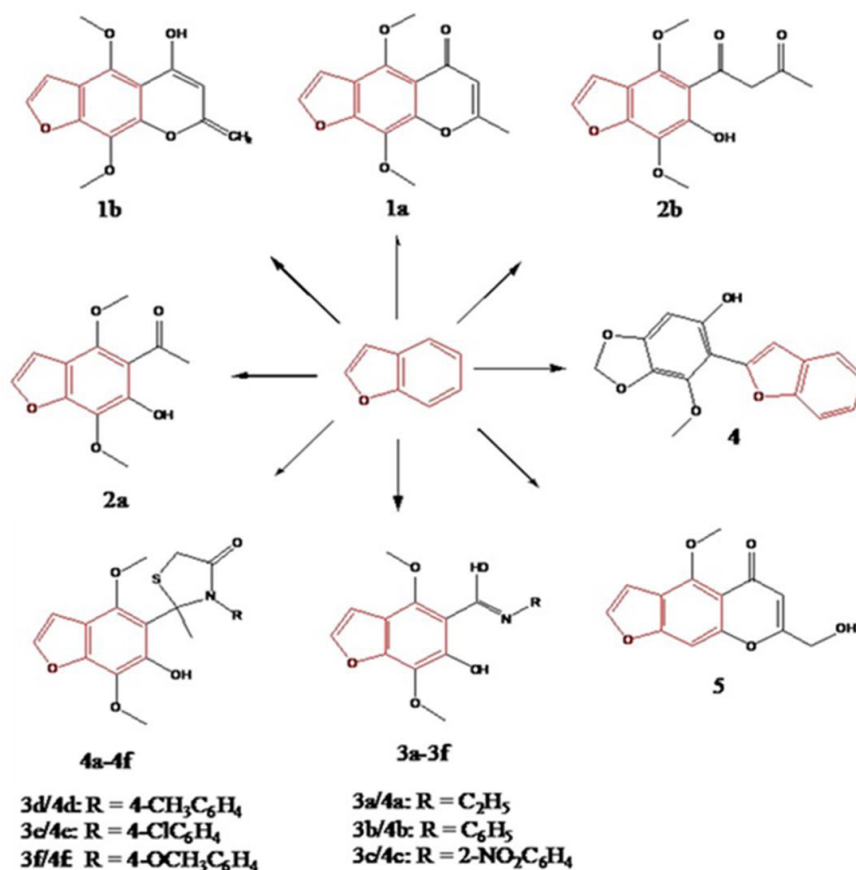


Figure 1: Molecular structures of the studied benzofuran derivatives

In this work, we wish to search for a theoretical model of the antioxidant activity of benzofuran derivatives [25] to help researchers better understand the phenomenon and better understand the design of new antioxidant drugs.

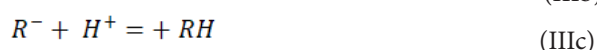
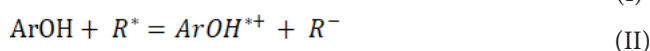
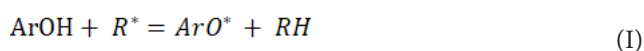
For this purpose, the physicochemical parameters such as bond dissociation enthalpy (BDE), ionization potential (IP), proton dissociation enthalpy (PDE), proton affinity (PA), and the electron transfer enthalpy (ETE) are calculated to explore the free radical scavenging mechanism. As a complement, frontier molecular orbital (HOMO, LUMO) and spin density of radicals were also analyzed.

Computational method

All calculations are carried out by using Gaussian09 software [26]. The geometries optimization and the calculation of the normal modes of vibration are performed at the level of the density functional theory (DFT) using the functionality B3LYP [27, 28] with the base 6-311G, in gas and solvated phases. Unrestricted calculations were performed for open-shell systems like radical species. Solvent effects (water, benzene, and DMSO) were taken into account using the self-consistent reaction field polarized continuum model (SCRF-PCM) [29, 30].

The ADME properties are calculated with ADMETlab 2.0 [31], available at: <https://admetmesh.scbdd.com>, and bioactivity studies are evaluated with Molinspiration online property calculation toolkit, available at <http://www.molinspiration.com>. To determine the most relevant descriptors of the antioxidant activity represented by the IC_{50} , a multi-linear regression analysis was carried out using Excel.

In the literature, three main antioxidant mechanisms are proposed and widely analyzed [32, 33] such as hydrogen atom transfer (HAT, **eq. (I)**), single-electron transfer followed by proton transfer (SET-PT, **eq. (II)**), and sequential proton loss electron transfer (SPLET, **eq. (III)**).



The physicochemical parameters BDE, IP, PDE, PA, and ETE were calculated using the following formulas:

$$\text{BDE} = \text{H}(\text{ArO}^*) + \text{H}(\text{H}^*) - \text{H}(\text{ArOH}) \quad (1)$$

$$\text{IP} = \text{H}(\text{ArOH}^{*+}) + \text{H}(\text{e}^-) - \text{H}(\text{ArOH}) \quad (2)$$

$$\text{PDE} = \text{H}(\text{ArO}^*) + \text{H}(\text{H}^+) - \text{H}(\text{ArOH}^{*+}) \quad (3)$$

$$\text{PA} = \text{H}(\text{ArO}^-) + \text{H}(\text{H}^+) - \text{H}(\text{ArOH}) \quad (4)$$

$$\text{ETE} = \text{H}(\text{ArO}^*) + \text{H}(\text{e}^-) - \text{H}(\text{ArO}^-) \quad (5)$$

where H(X) is the enthalpy of the X species [32].

Results and Discussion

HAT Mechanism

The O-H BDE appeared as a major descriptor in evaluating the structure-activity relationships for antioxidants [34] and it can also be associated with the SET-PT and SPLET mechanisms. This is so because the total energy requirements related to the SET-PT (sum of IP and PDE) and SPLET (sum of PA and ETE) mechanisms perfectly correlate with the BDE value [35] (see Figure. 2).

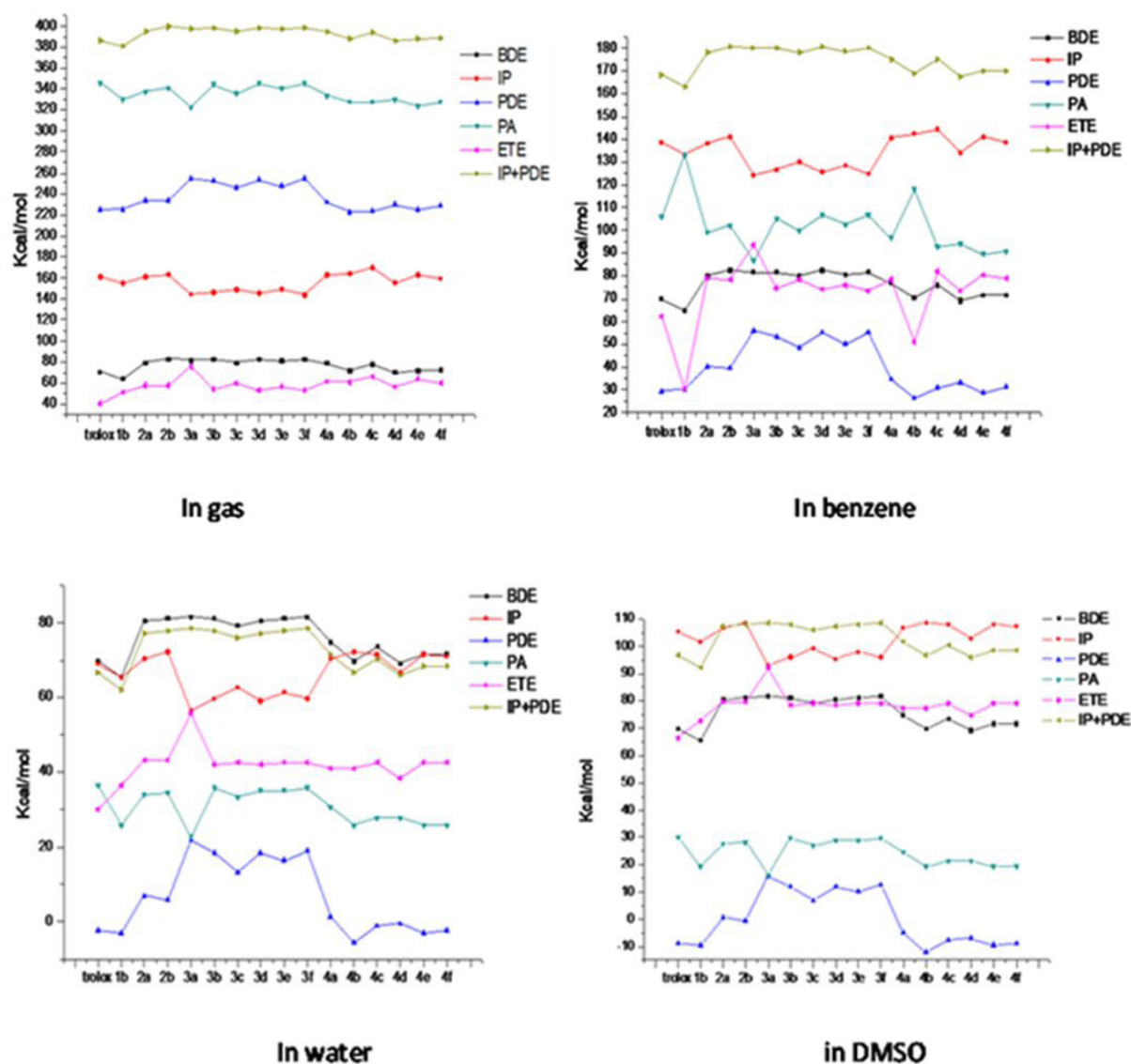


Figure 2: Calculated enthalpies (in gas, benzene, water, and DMSO) graphics

As shown in Table 1, Khellin (**1a**, keto form) may be inactive due to the lack of OH group (see Figure. 3), as well as the very wide BDEs of C₅-H in phenyl ring (113.07kcal/mol) and BDEs of C₇-H (86.72kcal/mol). This is in agreement with the experimental results [23].

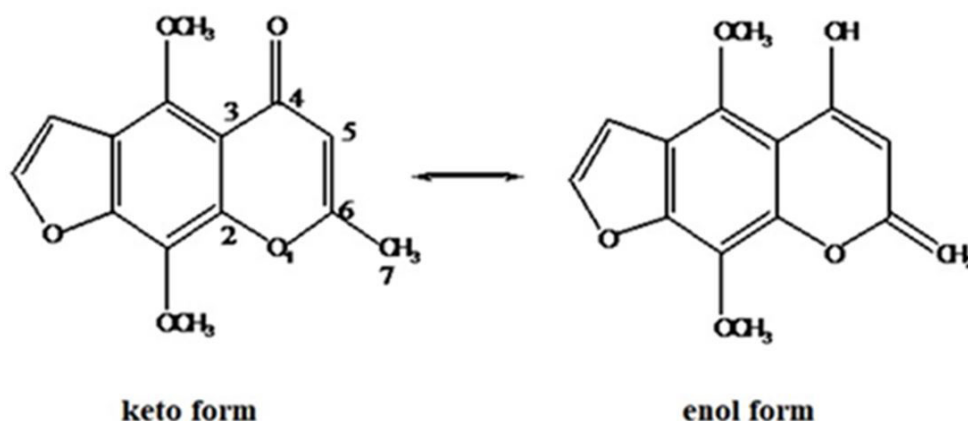


Figure 3: keto-enol tautomeric equilibrium

Theoretical properties	Gas-phase	Water	DMSO	Benzene
BDE(C ₅ -H)	113.07	113.70	113.70	113.07
BDE(C ₇ -H)	86.72	87.35	87.35	86.72
IP	158.25	69.03	105.39	136.79
PDE	244.35	15.06	8.78	48.31
E _{HOMO} (eV)	-5.71	-5.98	-5.97	-5.85
E _{LUMO} (eV)	-1.47	-1.72	-1.72	-1.57

Table 1: Theoretical properties of khellin (1a)

The gas phase HOMO energies are -5.71 eV for **1a** (keto form) and -5.44 eV for **1b** (enol form), with a BDE of the enol form which lower than that of Trolox by 64.13 kcal/ soft. As for compound **1a**, the difference is of the order of 6 (keto form), and 22 (enol form) kcal/mol, which shows that **1b** has greater mobility of its hydrogen. Furthermore, the gas phase IP values for **1a** and **1b** are 158.25kcal/mol and 155.2kcal/mol, respectively. So, all calculations show that **1b** is more nucleophilic than **1a** and thus the enol form is more reactive than the keto form.

Compounds	BDE in Gas	BDE in Water	BDE in DMSO	BDE in Benzene	IC ₅₀ (μM)
Trolox	70.41	69.78	69.78	69.78	5.42
1b	64.13	65.39	65.39	64.76	
2a	79.19	80.45	80.45	79.82	
2b	82.95	81.07	81.07	82.33	
3a	81.70	81.70	81.70	81.70	
3b	82.33	81.07	81.07	81.07	
3c	79.19	79.19	79.19	79.82	10.59
3d	82.33	80.45	80.45	82.33	9.72
3e	81.07	81.07	81.07	80.45	
3f	82.33	81.70	81.70	81.70	8.57
4a	78.56	74.80	74.80	76.68	
4b	71.66	69.78	69.78	70.41	
4c	77.93	73.54	73.54	76.05	
4d	69.78	69.15	69.15	69.15	8.27
4e	71.66	71.66	71.66	71.66	
4f	72.29	71.66	71.66	71.66	

Table 2: Calculated BDE values (kcal/mol) in the gas phase and different solvents for the studied benzofuran derivatives at the B3LYP /6-311G level

The bond dissociation enthalpy of O-H benzofuran derivatives in the gas and solvate phase are listed in Table 2. For the two hydrolyzed derivatives of khellin **2a** and **2b**, the BDEs are respectively 79.19 kcal/mol and 82.95 kcal/mol; they are higher than that of Trolox by about 9 and 12.5 Kcal/mol, respectively. Thus, **2a** and **2b** have less ability to donate protons than Trolox.

The BDE values of benzofuran Schiff base derivatives in the gas phase, illustrated in Table 2, are in the range of 79.19 - 82.33kcal/mol higher than those of benzofuran thiazolidinone derivatives (69.78 - 78.56kcal/mol). This indicates that benzofuran thiazolidinone derivatives are more potent antioxidants than benzofuran Schiff base derivatives.

The order of the BDEs of the series (**3a** to **3f**), in the gas phase, is **3b = 3d = 3f** > **3a** > **3e** > **3c**. So their H-donating abilities are in reverse order.

In water and DMSO solvents, the BDE values obey the same order of **3c** > **3d** > **3b = 3e** > **3a = 3f**. **3c** is the most active one among the studied benzofuran derivatives independent of the media, while **3f** is the least one.

The difference between calculated and experimental BDEs [23] is around 2kcal/mol. This is due, during the attack of the DPPH radical [36, 37], to the different steric effects present in the molecules, unlike Trolox.

The analysis of the structures of these benzofuran derivatives shows that intramolecular hydrogen bonding (IHB) can be established between the O-H and the neighboring C=N group [38]. The distances O-H and N...H in the gas phase and water are listed in Table 3.

Compound	d _{O-H} in Gas	d _{O-H} in Water	d _{N...H} in Gas	d _{N...H} in Water	Angle (O-H...N)
3c	1.01	1.02	1.62	1.59	147.14
3e	1.02	1.03	1.60	1.55	147.26
3b	1.02	1.04	1.59	1.54	147.55
3d	1.02	1.04	1.59	1.53	147.69
3f	1.02	1.04	1.59	1.53	147.61
3a	1.03	1.06	1.57	1.48	148.48

Table 3: hydrogen bonds O-H...N (in Å) for the benzofuran Schiff base derivatives in gas phase and in water

The order of the BDEs, **3c** > **3e** > **3a** > **3b = 3d = 3f** (see Table 3), is since the hydrogen bonds become increasingly stronger while passing from **3c** to **3f** and which are shorter, therefore stronger, than the sum of the Van der Waals radii involved in it [38].

The variation in hydrogen bond lengths is the same in the gas and hydrate phase except for compound **3a** which has a different structure with the absence of the phenyl group attached to N. It can be concluded that for these benzofuran derivatives, electron-withdrawing Groups (EWG) attached to π conjugated groups at the N position of the Schiff base decrease significantly the BDEs (**3c** and **3e**). By contrast, electron-donating groups (EDG) increase significantly the BDEs (**3d** and **3f**).

The BDEs order, in the gas phase, is **4a** > **4c** > **4f** > **4e = 4b = 4d**, for the series (**4a** to **4f**). Thus, their H-donating abilities are in reverse order. The same order is observed in all solvents. Accordingly, **4d** is predicted to be the most active among the benzofuran thiazolidinone derivatives studied independently of the medium, while **4a** is the least one.

These results are in agreement with the experiment [23]. The BDE of **4d** (69.78kcal/mol) is lower than that of Trolox by about 0.63kcal/mol. This result shows that **4d** possesses antioxidant properties comparable to those of Trolox. This order, **4d** > **4b = 4e** > **4f** > **4c** > **4a**, can be explained by the formation of Intramolecular Hydrogen Bonds (IHB) between, the phenolic hydrogen and the oxygen atom of the O-CH₃ group (compound **4a**, **4c**), with the neighboring C-N group (**4b**) or with the neighboring C-S group (**4d**, **4e**, **4f**) as shown in Figure. 4.

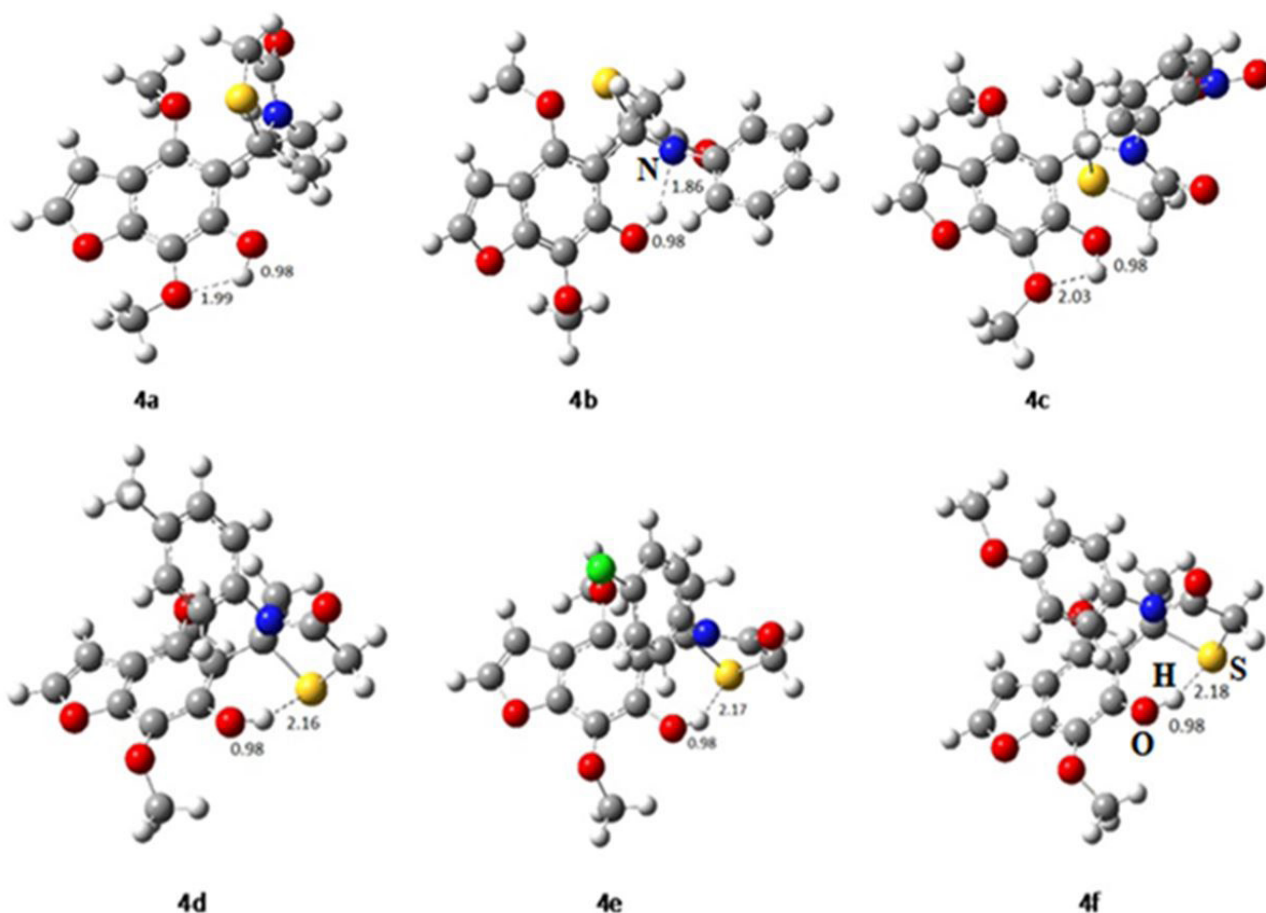


Figure 4: IHB in benzofuran thiazolidinone derivatives

Compound **4a** has the highest BDE (see Table 2) because its phenolic hydrogen is involved in a strong IHB with the oxygen of the -O-CH₃ group. Consequently, the strong BDE is because the elimination of the hydrogen atom implies the rupture of the IHB. **4d** has the lowest value because its hydrogen is involved in a weak IHB with the C-S group. The slight change in bond dissociation energies in different solvents is due to the absence of charged species in the HAT process.

The spin densities of the various radicals of benzofuran derivatives are shown in Figure 5. Their analysis helps us to better understand the differences in reactivity of the hydroxyl group (-OH) through the differences in BDE values. When the spin density of the radical is largely delocalized, the easier it forms and the lower its BDE value [39]. As can be seen in Figure 5, the spin densities of all the benzofuran derivatives studied are distributed over the phenolic oxygen atom and the benzofuran ring.

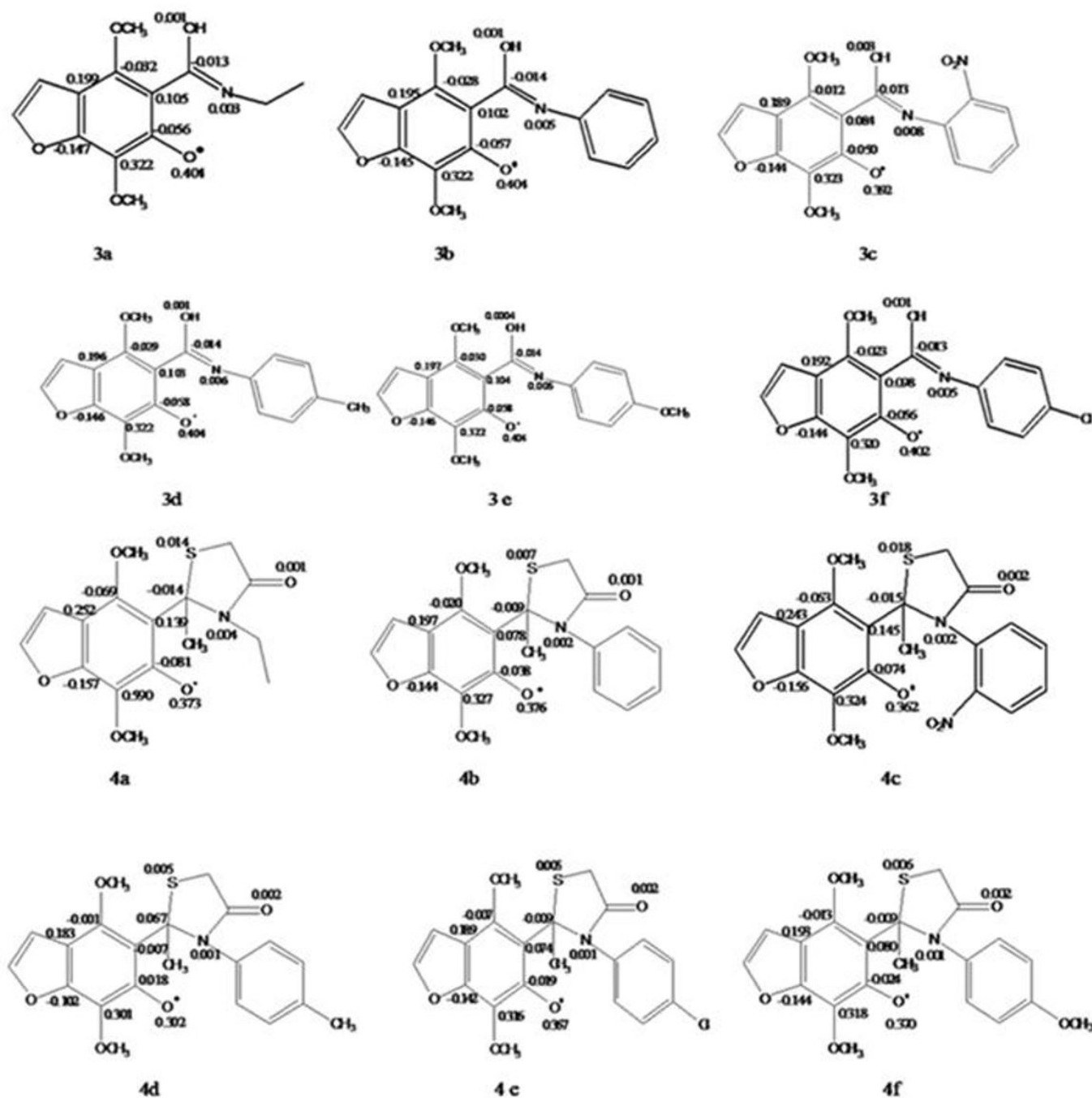


Figure 5: Spin density distribution of phenoxy radicals of the studied benzofuran derivatives

The spin densities of the oxygen atom are similar to that of benzofuran Schiff base derivatives (0.404). In **3c**, the spin density is substantially lower (0.392), so **3c** has low BDEs. This can explain why these radicals have similar BDE values and similar experimental results. Furthermore, it can be concluded that the different substituents at the N position do not affect the spin density distribution. For benzofuran thiazolidinone derivatives, **4d** possesses the lowest spin density (0.302) and **4b** the highest one (0.376). **4d** has the lowest BDE value among all the studied benzofuran derivatives.

SET-PT mechanism

Besides their involvement in the HAT mechanism, phenolic compounds can also scavenge free radicals by donating a single electron. The calculated IP and PDE values involved in the SET-PT mechanism in different solvents are reported in supplementary materials (see Tables S-1a, b, c, and d).

As can be seen, the gas phase IPs classification for the (3a-3f) series is $3f < 3a < 3d < 3b < 3c < 3e$ while in the benzene solvent it is $3a < 3f < 3d < 3b < 3e < 3c$ due to fact that the difference between 3f and 3a and between 3c and 3e does not exceed 1.25kcal/mol. In water and DMSO, the IPs is the same such as of $3a < 3d < 3b = 3f < 3e < 3c$. Compounds 3f and 3a have the strongest electron donating ability in the gas and solvated mediums, while 3c and 3e are the lowest ones.

For the series (4a to 4f), the order of the IP values is $4d < 4f < 4a = 4e < 4b < 4c$ in all media (see Tables S-1a, b, c and d). These results indicate that 4d is the most electron-donor than the others in all cases defined in Table S-1, while 4c has the lowest ones. These coherent predictions are generally in agreement with the results that can be deduced from the HOMO energies reported in Table 4.

Compounds	E _{HOMO} (eV)	E _{LUMO} (eV)
1b	-5.44	-1.41
3a	-5.59	-1.39
3b	-5.59	-1.71
3c	-5.75	-3.59
3d	-5.55	-1.65
3e	-5.72	-1.94
3f	-5.53	-1.61
4a	-5.82	-0.90
4b	-5.83	-1.28
4c	-6.12	-2.82
4d	-5.72	-0.75
4e	-6.06	-0.67
4f	-5.90	-1.12

Table 4: HOMO and LUMO energies for the studied benzofuran derivatives at the B3LYP /6-311G level

A comparison of the IPs of 3b and 3f shows that the first value is smaller than the second by about 2.5kcal/mol. This shows that the introduction of an electron donating group (EDG) is useful to reduce the value of its PI and thus improve the electron-donor power of the benzofuran derivatives studied. The same is true for 4b and 4d. Contrary to the BDEs values, the IPs obtained in a solvated medium, are significantly lower compared to those in the gas phase. This can be attributed to the stabilization undergone by charged systems in polar solvents [40]. For example, the IP value of the most active compound 3f decreases by 84kcal/mol when passing from gas to a hydrated state. These results indicate the importance of solvent polarity in controlling the SET-PT mechanism. Compound 3a has the highest PDE values in each medium, while 4d has the lowest value. Thus, 4b appears to be the most active in the deprotonation step. Since the cationic radical and the proton are charged species, solvent effects on PDE values are observed. Compared to the gas phase, deprotonation is easier, particularly in polar solvents such as water and DMSO.

As shown in supplementary materials (see Tables S-1a, b, c and d), the PIs values obtained for all the benzofuran derivatives (56.47 to 170.18 kcal/mol) are, for the most part, lower than those of Trolox (69.03 to 161.39 kcal/mol). This suggests that the benzofuran derivatives studied have an electron-donating ability greater than that of Trolox.

SPLET mechanism

SPLET mechanism has been reported as a possible pathway to trap radicals for antioxidants, especially in polar environments.

For the (3a- to 3f) series, the data analysis of Tables 4a, b, c, and d shows that the order of the AP values is, in all the environments defined in the same Tables, $3a < 3c < 3e < 3b < 3d = 3f$. For the series (4a to 4f), the order is $4e < 4b = 4c = 4f < 4d < 4a$. This shows that 3a and 4e are more deprotonated than the others.

The PAs values comparison of compounds 3b and 3e shows that the first value is smaller than the second one by about 4.4kcal/mol, which proves the effect of the electron-withdrawing Group (EWG) diminishes the PAs values and improves deprotonation.

The same is true for **4b** and **4e**. We also observe notable solvent effects on the values of the APs (see Tables S-1 a, b, c, and d in supplementary materials). For example, the PA value of **3a** goes from 322.16 kcal/mol (in the gas phase) to 86.59 (in benzene), 22.59 (in water), and 16.31 (in DMSO) kcal/mol, which is probably due to the high solvation enthalpy of the proton. This means that polar solvents promote the deprotonation of the species studied. The PA values of the benzofurans studied are significantly lower than those of Trolox. Thus, the deprotonation of the compounds is easier than in Trolox.

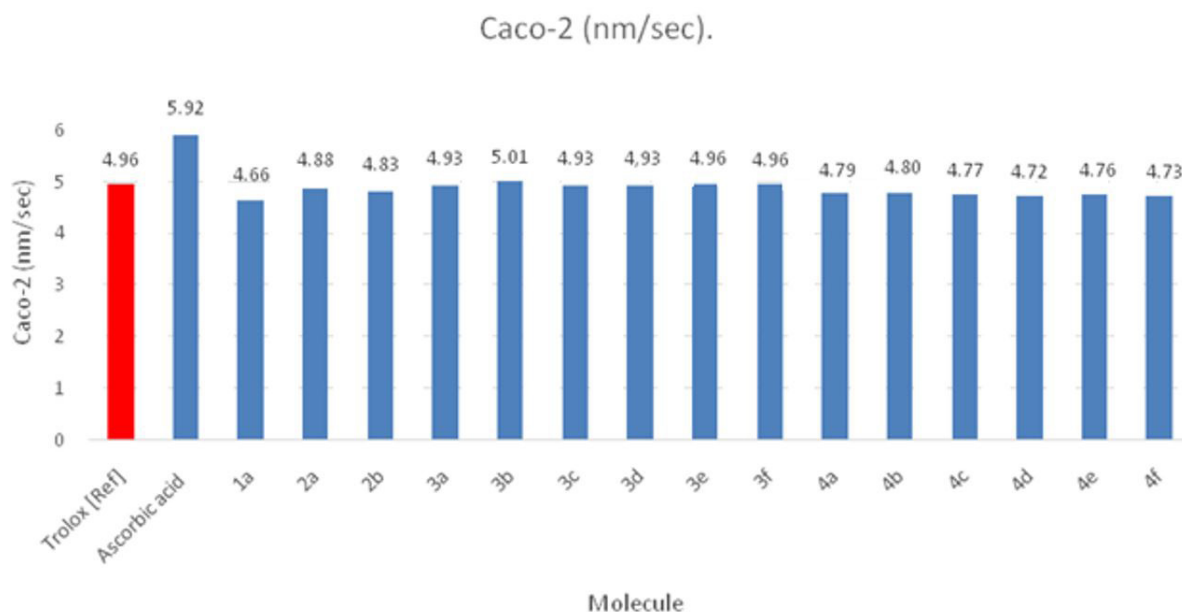
ADME Properties of studied compounds

Predicting Absorption, Distribution, Metabolism, and Excretion (ADME) properties of new drug candidates is critical to detect wile molecules are undesirable drug-like profiles. A drug in blood exists in two forms, bounded and unbounded. A portion of the drug becomes bound to plasma protein, the other part being unbound. The unbound form is being metabolized and/or excreted from the body whereas the bound part will be released to maintain equilibrium. The fraction unbound is the fraction that is active and may be excreted. For these, the plasma protein binding (PPB%) is an important pharmacokinetic factor [41] where the percentage of PPB classifies the compound as strongly bounded if $PPB \% > 90\%$ and may have a low therapeutic index (reduces its action as well as its efficacy).

On the other hand, predicting Human Intestinal Absorption (HIA %) of the drug is important to identify the potential drug candidate. HIA is the sum of bioavailability and absorption evaluated from ration or cumulative excretion in urine, bile, and excrement [42]. For a given compound, HIA% values that occur, in the range [0 to 0.3], indicate poor, in [0.3 to 0.7] average, and [0.7 to 1, 0] good intestinal absorption. On the other hand, Blood-brain barrier (BBB) penetration is an important pharmaceutical criterion. BBB penetration is presented as the concentration ratio of steady-state or radio-labeled compounds in a brain (C_{brain}) and peripheral blood (C_{blood}). The compounds which can pass the BBB are called Central Nervous System active (CNS-active) compounds ($BBB > 0.30$) and which are unable are called CNS-inactive compounds ($BBB < 0.30$). The human colon adenocarcinoma cell lines (Caco-2) as an alternative approach for the human intestinal epithelium, have been commonly used to estimate *in vivo* drug permeability due to their morphological and functional similarities. Compounds with a caco-2 value < -5.15 (logcm/s) are lower permeable and those with a value > -5.15 (logcm/s) are highly permeable and facilitate its penetration into cellular biochemical processes [43].

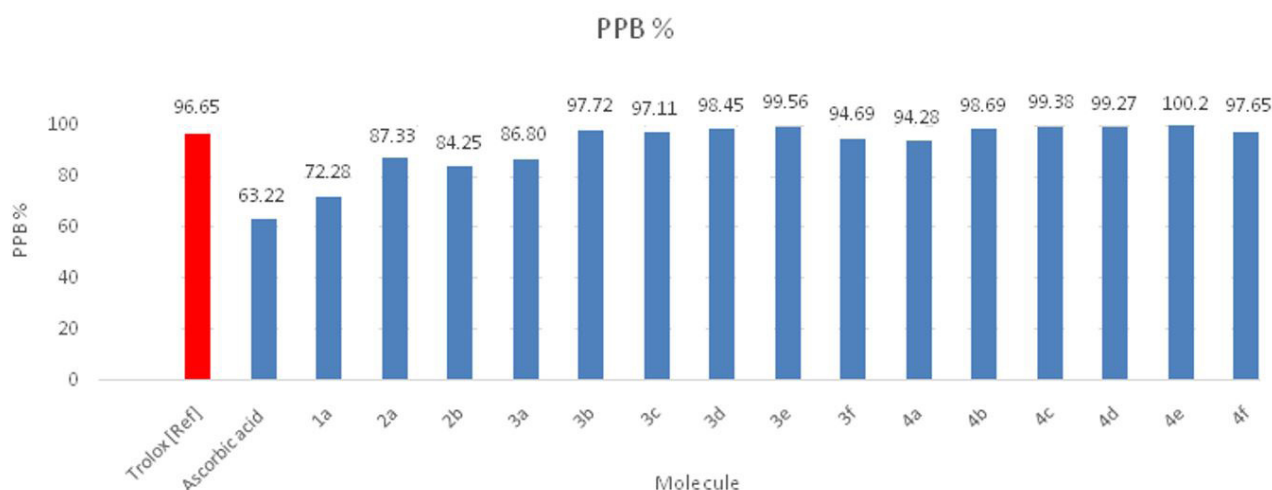
Furthermore, the apparent permeability coefficient (Papp) of the MDCK (Martin-Darby Canine Kidney) cell lines is also used to estimate the effect of the BBB index. An MDCK permeability value of less than 2.10^{-6} cm/s indicates that the compounds are low permeability, a value between [2 and 20.10^{-6}] cm/s indicates that the compounds are moderately permeable and a value greater than 20.10^{-6} cm/s indicates that the compounds have high MDCK permeability [44]. Thus, the Caco-2 and MDCK indexes are important for the eligibility of a drug candidate. The main drug targets are receptors, ion channels, nucleic acid, and transporters. So, the values of calculation of ion channel modulation (ICM), nuclear receptor ligand (NRL), bioactivity for G protein-coupled receptors ligand (GPCR), enzyme and kinase inhibition (EI) and (KI) respectively indicate binding affinity of the studied compounds to the receptors and enzymes. A negative value means low affinity, while a positive value indicates greater affinity [45]. The logarithm of the n-octanol/water distribution coefficient (log P), possesses a predominant position with an impact on both membrane permeability and hydrophobic binding to macromolecules. Compounds with values in the range [0 to 3] (log mol/l) will be considered good candidates. Finally, the logarithm of the aqueous solubility value (log S) is a good index that quantifies the absorption of the drug and its disintegration by its dissolution. It is of great importance in drug discovery. Compounds having values in the range [- 4 to 0.5] log(mol/l) will be considered good drug candidates.

Table 2, given in supplementary materials, shows that compounds **1a**, **2a**, **2b**, **3a**, and **4a** have, (log S) values of between -3.19 and -3,585 that correspond to molecules with good dissolution, and (log P) values of between 1,877 and 2.563 that correspond to good permeability and hydrophobic binding of these compound to macromolecules. The analysis of predicted ADME properties (see Tables S-2a and b) of studied compounds revealed the *in vivo* BBB penetration efficiency ranging from 0.028 to 0.501 cm/s. Compounds **3a**, **4a**, and **4c** ensure their level of CNS activity compared to Trolox or ascorbic acid with 0.153 and 0.073 respectively. The values of Caco-2 cell permeability ranged from -5.012 to -4.659 (nm/sec). All the studied compounds are highly permeable since the Caco-2 cell permeability is > -5.15 (logcm/s) (see histogram 1 and Tables S-2a and b).



Histogram 1: Caco-2cell permeability index as vs. compounds

This efficiency provides sustained permeability to bind with the plasma proteins. The PPB affinity values are in the range of 72.28 to 100.2%. Compounds **1a**, **2a**, **2b**, and **3a** have PPB affinity < 90% indicating that may be efficient. In contrast, compounds **3b - 3f** and **4a - 4f** have % PPB > 90% so, they may have a low therapeutic index (see histogram 2 and Tables S-2a and b).



Histogram 2: PPB% affinity as vs. compounds. All values are to be multiplied by (-1)

The MDCK cell permeability identified for them is ranging from $0.9 \cdot 10^{-5}$ to $3.0 \cdot 10^{-5}$ cm/s. The majority of compounds have MDCK cell permeability value $> 2.10^{-5}$ cm/s which indicates that they have passive MDCK cell permeability. The HIA % is ranging from 0.008 to 0.118 which means a good oral bioavailability for all the studied compounds.

The physicochemical properties of tested compounds represented in Table S-2 shows that they have a good pharmacokinetic profile and can be considered drug candidates since there are zero LIPINSKI property violations. The bioactivity study shows that all the studied compounds have negative value, which means low affinity and so they are not mutagenic or tumorigenic. Except for ICM value, compounds **2a**, **2b** and **4a** have positive values: 0.42, 0.36 and 0.54 respectively. This indicates that these three compounds can modulate ion channels (channel blockers or channel openers).

Multi-linear Regression (MLR) results

Because of the limited number of IC_{50} of the molecules studied in the present work (see Table 2), the MLR results should be treated as preliminary ones, however, various results could be concluded.

Correlation analysis revealed that the relationship between (IP + PDE), PA, and ETE descriptor calculated in water for the studied benzofuran derivatives at the B3LYP /6-311G level of theory, and IC₅₀ data gives the best following multi-linear regression:

$$IC_{50}(\mu M) = 0.563 + 148.25 * (IP + PDE) - 148.42 * PA - 147.89 * ETE$$

with a squared correlation coefficient equal to 0.99 and with a critical value of Fisher index (F) equal to 0.08; F-value is found statistically significant at 95% level.

Conclusion

In this study, the antioxidant activity of benzofuran Schiff base derivatives and benzofuran thiazolidinone derivatives were evaluated using DFT calculations. Several molecular descriptors (BDE, IP, PDE, PA, and ETE) associated with antioxidant action were calculated. Our results indicate that khellin (1a) is not a good antioxidant, but its enol form (1b) was found more potent than Trolox. The two hydrolyzed derivatives of khellin (2a) and (2b) were found to exhibit moderate antioxidant activity. The results indicate also that benzofuran thiazolidinone derivatives (4a - 4f) are better antioxidants than benzofuran Schiff base derivatives (3a - 3f), which is in good agreement with experimental results. From BDEs, 3c and 4d are the most active among the studied benzofuran derivatives independent of the media, while 3f and 4a are the poorest. From IPs, 3a, 3f, and 4d are more prone to donate electrons than others in all four media, while 3c, 3e, and 4c are the least effective. From PAs, 3a and 4e are more prone to deprotonation than others.

By comparing the values of parameters reported in Tables 2, S-1, 4, and S-2, it appears that the BDEs are much lower than the IPs and PAs in the gas phase and benzene solution. This indicates that the HAT process should be more prone to occur than SET-PT and SPLET mechanism in the gas phase and nonpolar media. In the studied environments, the calculated IPs for all the studied benzofuran derivatives are significantly higher than the BDEs and PAs in all the media except for water when IPs are lower than BDEs but higher than the PAs. Thus, the SET-PT mechanism is the least favored in the studied environments. With the increase of solvent polarity, PAs greatly decrease and became significantly lower than BDEs and IPs in DMSO and water solutions, which makes SPLET more favorable in polar media. A comparison of BDEs of the studied benzofuran derivatives, with no substituted one, indicates that electron-withdrawing groups (EWG) attached to π conjugated groups at the N position decrease BDEs. On the contrary, electron-donating groups (EDG) reduce BDEs values. Also, EDG is helpful to decrease the IP and thus enhances the electron-donating ability of the studied benzofuran derivatives. On the contrary, the introduction of EWG is helpful to decrease the PAs and thus enhance deprotonation.

Notably, in each environment (gas or solvated phases), IP+PDE and PA+ETE are perfectly correlated with BDE. The above results rationalize the antioxidant effect of these benzofuran derivatives, which will provide valuable information for the design and synthesis of a new powerful antioxidant.

References

1. Andreescu S, Hpel M (2011) Oxidative Stress : Diagnostics, Prevention, and Therapy ACS Symposium Series.
2. Valko M, Leibfritz D, Moncol J, Cronin MTD, Mazur M, et al. (2007) Free radicals and antioxidants in normal physiological functions and human disease., *Int. J Biochem Cell Biol* 39: 44-84.
3. Fang Y-Z, Yang S, Wu G (2002) Free radicals, antioxidants, and nutrition. *Nutrition* 18: 872-79.
4. Fritz KL, Seppanen CM, Kurzer MS, Csallany Saari A (2003) The in vivo antioxidant activity of soybean isoflavones in human subjects. *Nutr Res* 23: 479-87.
5. Oteiza P I, Erlejman AG, Verstraeten SV, Keen CL, Fraga CG (2005) Flavonoid-membrane interactions: A protective role of flavonoids at the membrane surface? *Clin Dev Immunol* 12 : 592035.
6. Khanam H (2015) Bioactive benzofuran derivatives : A review *Eur J Med Chem* 97 : 483-504.
7. Narimatsu S, Tachemi C, Kuramoto S, Tsuzuki D, Hichiya H, et al. (2003) Stereoselectivity in the oxidation of bufuralol, a chiral substrate, by human cytochrome P450s. *Chirality* 15: 333-39,
8. Cheng HC, Ulane CM, Burke RE (2010) Clinical progression in parkinson disease and the neurobiology of axons. *Ann Neurol* 67: 715-25,
9. González-Gómez JC, Santana L, Uriarte E (2005) A furan ring expansion approach to the synthesis of novel pyridazino-psoralen derivatives. *Tetrahedron* 61: 4805-10.
10. Koca M, Servi S, Kirilmis C, Ahmedzade M, Kazaz C, et al (2005) Synthesis and antimicrobial activity of some novel derivatives of benzofuran : Part 1. Synthesis and antimicrobial activity of (benzofuran-2-yl) (3- phenyl-3-methylcyclobutyl) ketoxime derivatives. *Eur J Med Chem* 40: 1351-8,
11. Kao CL, Chern JW (2001) A convenient synthesis of naturally occurring benzofuran aianthoidol. *Tetrahedron Lett* 42: 1111-13,
12. Naik R, Harmalkar D S, Xu X, Jang K, Lee K (2015) Bioactive benzofuran derivatives : Moracins A - Z in medicinal chemistry. *Eur J Med Chem* 90: 379-93.
13. He S, Jain P, Lin B, Ferre M, Hu Z, et al. (2015) High-throughput screening, discovery, and optimization to develop a benzofuran class of hepatitis C virus inhibitors. *ACS Comb Sci* 17: 641-52.
14. Verma A, Saraf SK (2008) 4- thiazolidinone : a biologically active scaffold. *Eur J Med Chem* 43: 897-905.
15. Tripathi AC, Gupta SJ, Fatima G N, Sonar PK, Verma A, et al (2014) 4-Thiazolidinones : the advances continue *Eur J Med Chem* 72: 52-77.
16. Pires Gouvea D, Vasconcellos FA, Berwaldt G dos A, Pinto Seixas Neto AC, Fischer G, et al (2016) 2-Aryl-3-(2-morpholinoethyl) thiazolidin-4- ones: Synthesis, anti-inflammatory in vivo, cytotoxicity in vitro and molecular docking studies. *Eur J Med Chem* 118: 259-65.

17. Barreca ML, Balzarini J, Chimirri A, De Clercq E, De Luca L, et al. (2002) Design, synthesis, structure - Activity relationships, and molecular modeling studies of 2,3-diaryl-1,3-thiazolidin-4-ones as potent anti-HIV agents. *J Med Chem* 45, 24: 5410-13.
18. Rao A, Balzarini J, Carbone A, Chimirri A, De Clercq A, et al. (2004) 2-(2,6-Dihalophenyl) -3-(pyrimidin-2-yl) -1,3-thiazolidin-4-ones as non-nucleoside HIV-1 reverse transcriptase inhibitors, *Antiviral Res* 63:79-84.
19. Rawal RK., Tripathi R, Katti SB, Pannecouque C, De Clercq E (2007) Synthesis and evaluation of 2-(2,6-dihalophenyl) -3-pyrimidinyl-1,3-thiazolidin-4-one analogues as anti-HIV-1 agents. *Bioorganic Med Chem* 15, 9 : 3134-42.
20. De Siqueira LRP, De Moraes Gomes PAT, De Lima Ferreira LP, De Melo Rêgo M J B, Leite A C L (2019) Multi-target compounds acting in cancer progression : Focus on thiosemicarbazone, thiazole and thiazolidinone analogues. *Eur J Med Chem* 170: 237-60.
21. El-khouly OA, Henen MA., El-sayed M A, Shabaan MI, El-messery S M (2021) Synthesis, anticancer and antimicrobial evaluation of new benzofuran based derivatives : PI3K inhibition, quorum sensing and molecular modeling study. *Bioorg Med Chem* 31:115976.
22. Hwu JR, Gupta N K, Tsay S-C, Huang W-C, Albulescu I C, et al. (2017) Bis(benzofuran-thiazolidinone) s and Bis(benzofuran-thiazinanone) s as inhibiting agents for chikungunya virus. *Antiviral Res* 146: 96-101.
23. Latif NA A, Abdel SH, Break LM (2013) Synthesis of new benzofuran 1, 3 thiazolidin 4 one derivatives from natural sources and study of their antioxidant activity. *Russ J Bioorganic Chem* 39: 438-443.
24. Chand K, Hiremathad A, Singh M, Santos MA, Keri RS (2016) A review on antioxidant potential of bioactive heterocycle benzofuran : Natural and synthetic derivatives. *Pharmacological Reports* 69: 281-95.
25. Ati F, Chergui A, Aboul-Enein HY, Maouche B (2018) Antioxidant activity of some khellin derivatives: a density functional theory study. *Egypt Pharm J* 17: 212-17.
26. Frisch MJ, Trucks GW, Schlegel HB, Scuseria GE, Robb M A, et al., (2009) Gaussian 09 Revision A.2.
27. Becke A D (1993) Density-functional thermochemistry. III. The role of exact exchange. *J Chem Phys* 98: 5648-52.
28. Lee C, Yang W, Parr RG (1988) Development of the colle-salvetti correlation-energy formula into a functional of the electron density. *Phys Rev B* 37: 785-89.
29. Tomasi J, Mennucci B, Cammi R (2005) Quantum mechanical continuum solvation models. *Chem Rev* 105: 2999-3093.
30. Barone V, Cossi M, Tomasi J (1997) A new definition of cavities for the computation of solvation free energies by the polarizable continuum model. *J Chem Phys* 107:3210.
31. Xiong G, Wu Z, Yi J, Fu L, Yang Z, et al. (2021) ADMET lab 2.0: An integrated online platform for accurate and comprehensive predictions of ADMET properties. *Nucleic Acids Res* 2 : W5-W14.
32. Galano A (2015) Free radicals induced oxidative stress at a molecular level : The current status, challenges and perspectives of computational chemistry based protocols. *J Mex Chem Soc* 59: 231-62.
33. Leopoldini M, Russo N, Toscano M (2011) The molecular basis of working mechanism of natural polyphenolic antioxidants. *Food Chem* 125: 288-306.
34. Wright JS, Johnson ER, Dilabio GA (2001) Predicting the activity of phenolic antioxidants : Theoretical method, analysis of substituent effects, and application to major families of antioxidants. *J Am Chem Soc* 123:1173-83.

35. Amic D, Lucic B (2013) H bond dissociation enthalpy effectively represent free radical scavenging PM6 study of free radical scavenging mechanisms of flavonoids : why does O-H bond dissociation enthalpy effectively represent free radical scavenging activity ? *J Mol Model* 19: 2593-2603.
36. Schaich K M, Tian X, Xie J (2015) Hurdles and pitfalls in measuring antioxidant efficacy: A critical evaluation of ABTS, DPPH, and ORAC assays. *J Funct Foods* 14:111-25.
37. Foti M C (2015) Use and abuse of the DPPH • radical. *J Agric Food Chem* 63: 8765-76.
38. Buemi G (2006) Intramolecular hydrogen bonds. Methodologies and strategies for their strength Evaluation. In : Grabowski S J eds) *Hydrogen Bonding—New Insights*, Springer Dordrecht 3 :51-107.
39. Leopoldini M, Pitarch IP, Russo N., Toscano M (2004) Structure, conformation and electronic properties of aligenin, Luteolin and taxifolin antioxidants. A First Principle Theoretical Study. *J Phys Chem A* 108: 9-96.
40. Nenadis N, Tsimidou M Z (2012) Contribution of DFT computed molecular descriptors in the study of radical scavenging activity trend of natural hydroxybenzaldehydes and corresponding acids. *food Res Int* 48:538-43.
41. Yuan Y, Chang S, Zhang Z, Li Z, Li S, et al. (2020) A novel strategy for prediction of human plasma protein binding using machine learning techniques. *Chemom Intell Lab Syst* 199: 103962.
42. Wang N, Huang C, Dong J, Yao Z, Zhu M (2017) Predicting human intestinal absorption with modified random forest approach: a comprehensive evaluation of molecular representation, unbalanced data, and applicability domain issues. *RSC Adv* 7 :19007-18.
43. Shaker B, Yu M S, Song JS, Ahn S, Ryu JY, et al., (2020) LightBBB : Computational prediction model of blood-brain- barrier penetration based on LightGBM, *Bioinformatics* 37:1135-39.
44. Irvine J D, Takahashi L, Lockhart K, Cheong J, Tolan JW, et al. (1999) MDCK (Madin – Darby Canine Kidney) Cells : A tool for membrane permeability screening. *J Pharm Sci* 88: 28-33.
45. Bockaert J, Claeysen S, Bécamel C, Pinloche S, Dumuis AG (2002) Protein-coupled receptors: Dominant players in cell-cell communication. *Int Rev Cytol* 212: 63-132.

Supplementary Materials

Table S-1: Calculated IP, PDE, PA, ETE, and (IP+PDE) values (kcal/mol) for the studied benzofuran derivatives at the B3LYP/6-311G level, (a) in the gas phase, (b) in benzene, (c) in DMSO and (d) in water

(a)

Compound	IP	PDE	PA	ETE	IP+PDE
Trolox	161.39	224.90	346.00	40.29	386.29
1b	155.12	225.52	329.69	50.95	380.64
2a	161.39	233.68	337.22	57.85	395.07
2b	163.27	233.68	340.98	57.85	398.83
3a	144.45	254.64	322.16	75.42	397.58
3b	146.33	251.88	344.12	54.09	398.21
3c	148.84	246.23	335.34	59.74	395.07
3d	145.08	253.13	345.38	52.83	398.21
3e	149.47	247.49	340.36	56.60	396.96
3f	143.82	254.39	354.38	52.83	398.21
4a	162.65	231.80	333.45	60.99	394.45
4b	164.53	223.01	327.81	60.49	387.54
4c	170.18	223.64	327.81	66.01	393.82
4d	155.74	229.93	329.69	55.97	385.67
4e	162.65	224.90	323.41	64.13	387.55
4f	159.51	228.66	327.81	60.36	388.17

(b)

Compound	IP	PDE	PA	ETE	IP+PDE
Trolox	138.68	29.49	106.05	62.12	168.17
1b	133.03	30.12	133.03	30.12	163.15
2a	138.05	40.16	99.14	79.06	178.21
2b	141.19	39.53	102.28	78.44	180.72
3a	124.24	55.85	86.59	93.50	180.09
3b	126.75	53.34	105.42	74.67	180.09
3c	129.89	48.32	99.77	78.44	178.21
3d	125.50	55.22	106.67	74.04	180.72
3e	128.64	50.20	102.91	75.93	178.84
3f	124.87	55.22	106.67	73.42	180.09
4a	140.56	34.51	96.63	78.44	175.07
4b	142.44	26.35	117.97	50.83	168.80
4c	144.32	30.75	92.87	82.20	175.07
4d	134.28	33.26	94.12	73.42	167.54
4e	141.19	28.86	89.73	80.32	170.05
4f	138.68	31.37	90.99	79.06	170.05

(c)

Compound	IP	PDE	PA	ETE	IP+PDE
Trolox	105.42	-8.79	30.12	66.52	96.63
1b	101.66	-941	19.45	72.79	92.25
2a	106.67	0.63	27.61	79.69	107.30
2b	108.56	-0.63	28.24	79.69	107.93
3a	92.87	15.69	16.31	92.24	108.56
3b	96.01	11.92	29.49	78.44	107.93
3c	99.14	6.90	26.98	79.06	106.04
3d	95.38	11.92	28.86	79.06	108.56
3e	97.89	10.04	28.86	79.06	107.93
3f	96.01	12.55	29.49	79.06	108.56
4a	106.67	-5.02	24.47	77.18	101.65
4b	108.56	-11.92	19.45	77.18	96.64
4c	107.93	-7.53	21.33	79.06	100.40
4d	102.91	-6.90	21.33	74.67	96.01
4e	107.93	-9.41	19.45	79.06	98.52
4f	107.30	-8.78	19.45	79.06	98.52

(d)

Compound	IP	PDE	PA	ETE	IP+PDE
Trolox	69.03	-2.51	36.40	30.12	66.52
1b	65.26	-3.14	25.73	36.40	62.12
2a	70.28	06.90	33.88	43.30	77.18
2b	72.16	05.65	34.51	43.30	77.81
3a	56.47	21.96	22.59	55.84	78.43
3b	59.61	18.20	35.77	42.04	77.81
3c	62.75	13.18	33.26	42.67	75.93
3d	58.98	18.20	35.14	42.04	77.18
3e	61.49	16.31	35.14	42.67	77.80
3f	59.61	18.82	35.77	42.67	78.43
4a	70.20	01.25	30.75	40.79	71.53
4b	72.16	-5.65	25.73	40.79	66.51
4c	71.53	-1.25	27.61	42.67	70.28
4d	66.51	-0.63	27.61	38.28	65.88
4e	71.53	-3.14	25.73	42.67	68.39
4f	70.91	-2.51	25.73	42.67	68.40

Table S-2: Predicted ADME and physicochemical properties of compounds

(a)

Molecule	PPB%	BBB (Cbrain/Cblood)	HIA%	Caco-2 (nm/s)	MDCK 10 ⁵ (nm/s)	GPCR	ICM
Trolox	96.65	0.153	0.013	-4.959	2.1	0.17	0.20
Ascorbic acid	63.22	0.073	0.069	-5.917	14.3	-0.53	-0.24
1a	72.28	0.052	0.025	-4.659	3.0	-0.36	0.16
2a	87.33	0.111	0.024	-4.881	2.1	-0.39	0.42
2b	84.25	0.080	0.030	-4.834	1.9	-0.23	0.36
3a	86.80	0.501	0.024	-4.931	9.0	-0.54	-0.06
3b	97.72	0.189	0.008	-5.012	1.6	-0.33	-0.05
3c	97.11	0.051	0.013	-4.931	2.8	-0.41	-0.18
3d	98.45	0.120	0.012	-4.925	1.2	-0.35	-0.12
3e	99.56	0.073	0.011	-4.957	1.5	-0.32	-0.05
3f	94.69	0.078	0.012	-4.964	1.2	-0.31	-0.06
4a	94.28	0.356	0.118	-4.785	1.7	-0.18	0.54
4b	98.69	0.057	0.038	-4.797	2.2	-0.34	0.09
4c	99.38	0.378	0.092	-4.766	2.5	-0.44	0.01
4d	99.27	0.056	0.072	-4.724	1.9	-0.36	0.03
4e	100.2	0.064	0.043	-4.764	2.0	-0.33	0.09
4f	97.65	0.028	0.041	-4.733	2.1	-0.33	0.07

(b)

Molecule	KI	NRL	PI	EI	Log (P)	Log (S)
Trolox	0.47	0.91	0.10	0.48	2.957	-2.922
Ascorbic acid	-1.09	-1.01	-0.81	0.20	-1.42	-0.613
1a	-0.51	-0.51	-0.64	-0.07	2.563	-3.556
2a	-0.65	-0.57	-0.79	-0.07	2.368	-3.190
2b	-0.63	-0.25	-0.49	0.22	1.877	-3.394
3a	-0.77	-0.81	-0.87	-0.28	2.213	-3.027
3b	-0.44	-0.50	-0.66	-0.26	3.576	-4.438
3c	-0.66	-0.71	-0.78	-0.35	3.360	-4.253
3d	-0.47	-0.50	-0.68	-0.31	4.020	-4.784
3e	-0.44	-0.49	-0.66	-0.29	4.272	-4.747
3f	-0.42	-0.43	-0.59	-0.25	3.649	-4.674
4a	-0.70	-0.69	-0.58	-0.31	2.515	-3.585
4b	-0.66	-0.64	-0.56	-0.32	3.395	-4.430
4c	-0.76	-0.81	-0.67	-0.39	3.268	-4.442
4d	-0.68	-0.64	-0.59	-0.36	3.823	-4.744
4e	-0.66	-0.64	-0.58	-0.34	4.070	-4.726
4f	-0.63	-0.58	-0.53	-0.31	3.396	-4.512